


Challenges and Opportunities in 3D Printing of Biodegradable Medical Devices by Emerging Photopolymerization Techniques

Journal Article**Author(s):**

Bao, Yinyin; Paunović, Nevena; [Leroux, Jean-Christophe](#) 

Publication date:

2022-04-11

Permanent link:

<https://doi.org/10.3929/ethz-b-000530255>

Rights / license:

[Creative Commons Attribution 4.0 International](#)

Originally published in:

Advanced Functional Materials 32(15), <https://doi.org/10.1002/adfm.202109864>

Funding acknowledgement:

177178 - 3D printing manufacturing of patient-tailored drug releasing stents (SNF)

Challenges and Opportunities in 3D Printing of Biodegradable Medical Devices by Emerging Photopolymerization Techniques

Yinyin Bao,* Nevena Paunović, and Jean-Christophe Leroux*

Since the first report of 3D printed biodegradable structures by stereolithography, vat photopolymerization has shown great potential in the fabrication of medical implants and devices. Despite its superior printing quality and manufacturing speed, the development of biodegradable devices by this technique remains challenging. This results from the conflicting viscosity requirements for the printing resins, i.e., low viscosity is required for high-resolution 3D printing, whereas high viscosity is often needed to provide high mechanical strength. Recently emerging photopolymerization-based 3D printing techniques, including heat-assisted digital light processing (DLP) and volumetric printing, have brought new hope to the field. With its tolerance to high viscosity resins, heat-assisted DLP enables the fabrication of complex, personalized architectures from biodegradable photopolymers that are not printable by conventional printing techniques. On the other hand, volumetric printing, which abandons the layer-by-layer printing principle and thus circumvents the dependence on low viscosity resins, could be highly beneficial for the 3D printing of biodegradable devices. This perspective evaluates the key challenges associated with biodegradable photopolymers used in the 3D printing of medical implants and devices. One focuses on their chemical structures and physical properties and discusses future directions offered by these emerging techniques.


1. Introduction

Implantable medical devices can have diagnostic, therapeutic, and/or regenerative functions in a wide range of clinical applications,^[1] such as vital signs monitoring,^[2] percutaneous coronary intervention,^[3] tracheal stenting,^[4] drug delivery,^[5] bone repair,^[6] and tissue regeneration.^[7] For certain applications,

biodegradable implantable devices that can be cleared from the body in a safe manner are desirable,^[8] as they spare the need for a second surgery that is otherwise necessary to remove nondegradable systems made, for instance, from silicone or metal.^[9] Moreover, the performance as well as the tolerance of medical devices can be improved by carefully adjusting the design parameters to the anatomophysiology of the patient.^[10] To produce such biodegradable, patient-tailored devices, advanced manufacturing techniques with high precision and speed are needed.

3D printing, or additive manufacturing, allows fabricating complex architectures in a rather efficient and straightforward manner.^[11–13] Among the current 3D printing techniques, vat photopolymerization is increasingly attracting attention due to its superior spatiotemporal resolution and fine surface finish.^[14–16] In particular, photopolymerization-based 3D printing, including stereolithography (SLA),^[17,18] digital light processing (DLP),^[19,20] and continuous liquid interface production (CLIP),^[21,22] holds great potential in biomedical applications.^[23,24] Since the first report in 2000,^[25] it has been shown that biodegradable photopolymers can be used to 3D print on-demand patient-specific resorbable devices when combined with imaging techniques such as computed tomography (CT). Despite the enormous potential of photopolymerization, the majority of degradable 3D printed devices are still prepared by extrusion-based additive manufacturing such as fused deposition modeling (FDM), which suffers from relatively low resolution.^[26] This is partially caused by the lack of suitable biomedical 3D printing resins that have the desired viscosity, and can simultaneously provide sufficient mechanical performance and bioactivity after printing (Figure 1). For instance, photopolymer chain length and reactive diluent concentration are both associated with the crosslinking network. As most photopolymers are functionalized at the chain end (e.g., methacrylate), the shorter polymer chain can provide a higher crosslinking degree and thus reduce the degradability. On the other hand, the addition of reactive diluents can increase the non-degradable part of the crosslinking product, as reactive diluents are usually vinyl-based monomers. In this perspective article rather than giving a comprehensive overview of 3D printing, we

Y. Bao, N. Paunović, J.-C. Leroux
Institute of Pharmaceutical Sciences
Department of Chemistry and Applied Biosciences
ETH Zurich
Vladimir-Prelog-Weg 1-5/10, Zurich 8093, Switzerland
E-mail: yinyin.bao@pharma.ethz.ch; jleroux@ethz.ch

 The ORCID identification number(s) for the author(s) of this article can be found under <https://doi.org/10.1002/adfm.202109864>.

© 2022 The Authors. Advanced Functional Materials published by Wiley-VCH GmbH. This is an open access article under the terms of the Creative Commons Attribution License, which permits use, distribution and reproduction in any medium, provided the original work is properly cited.

DOI: 10.1002/adfm.202109864

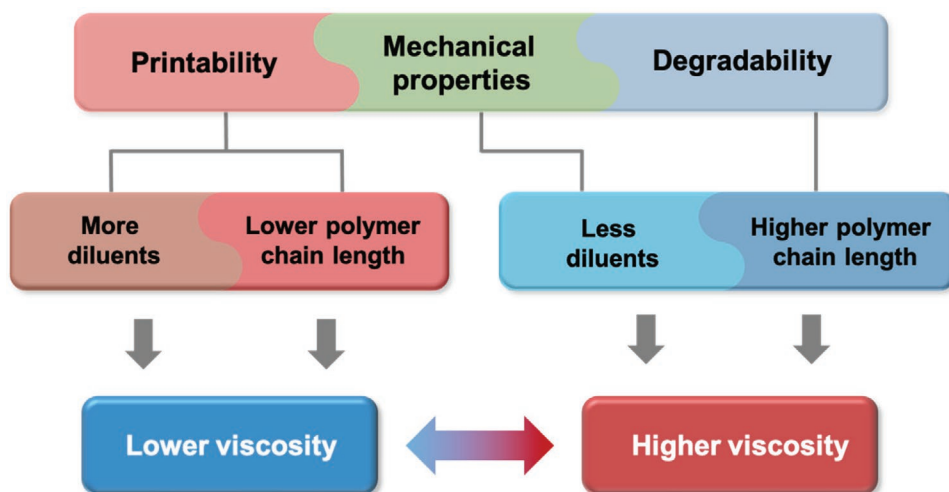


Figure 1. The antagonism between the low viscosity of the resin required for high-resolution 3D printing and the high viscosity resulting from high molecular weight photopolymers that can provide 3D printed objects with the desired mechanical properties and biodegradability.

focus on the key challenges associated with biodegradable photopolymers for 3D printed medical implants and devices, and explore the new opportunities brought by recently emerging techniques such as heat-assisted vat photopolymerization^[27–29] and volumetric 3D printing (Figure 2).^[30–34] Finally, we provide an outlook on the possible future research directions involving material design and technical progress.

2. Common Vat Photopolymerization Techniques

SLA was the first 3D printing technique to use vat photopolymerization. It was independently developed by Chuck Hull and Alain Le Mehaute in 1980s.^[35] SLA is based on localized photopolymerization activated by a single laser beam. It takes place in a bath containing liquid photocurable resin with low viscosity, composed of photopolymers or monomers and photoinitiators.

Following a vertical layer-by-layer crosslinking, which is typically triggered by the photolysis of the photoinitiator into the primary radicals or cations, the photocurable resin is converted to solid products.^[17,18] DLP relies on the same principle as SLA but further employs a digital micromirror device (DMD) that converts the laser beam to defined dynamic patterns (Figure 2a). Compared to SLA, this light projection function enables shorter crosslinking times for each layer.^[19,20] However, DLP is still limited in speed due to the lift-up step of the print head that is needed to enable the resin to flow back after each printed layer.

In 2015, DeSimone and co-workers introduced an oxygen-permeable window under the resin, and generated a dead zone for photopolymerization due to the oxygen inhibition of free radicals.^[21] The so-called CLIP 3D printing circumvented the main time-consuming step by allowing continuous additive manufacturing, drastically speeding up the vat photopolymerization. Recently, the Mirkin group established large-scale

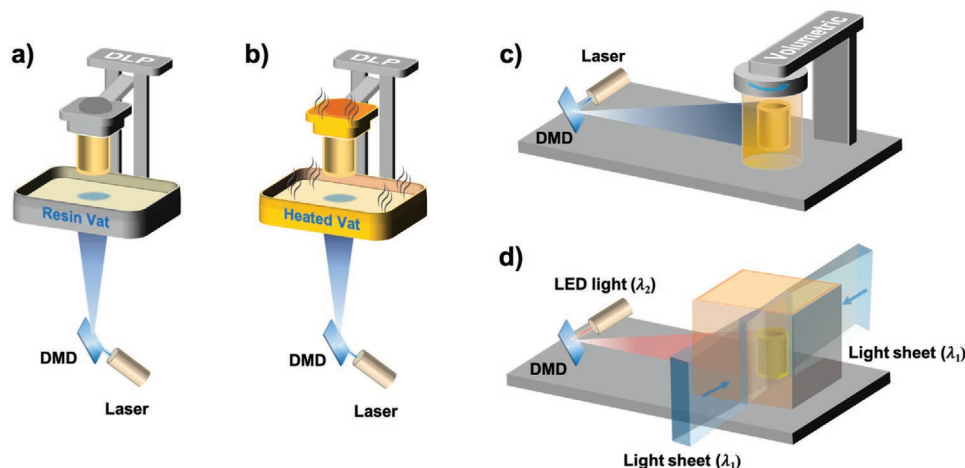


Figure 2. Working principle of a) conventional DLP, b) heat-assisted DLP (hot lithography). Reproduced under the terms of the CC-BY-NC-ND license.^[36] Copyright 2021, The Authors, published by American Chemical Society, c) tomographic volumetric printing (computed axial lithography). Reproduced with permission.^[31] Copyright 2019, The American Association for the Advancement of Science, and d) linear volumetric printing (xolography). Reproduced with permission.^[34] Copyright 2020, Springer Nature.

continuous 3D printing by introducing a fluorinated oil as the mobile liquid interface under the resin.^[37] Up until now, a variety of 3D printable photopolymers have been developed for SLA, DLP, CLIP, and their derived techniques. Although rapid 3D printing using conventional nonbiodegradable resins has been realized, vat photopolymerization manufacturing of biodegradable implantable devices remains challenging. This stems from the antagonism between the low viscosity of the resin required for high-resolution 3D printing and the high viscosity created by high molecular weight photopolymers needed to produce 3D printed devices with the desired mechanical properties and biodegradability (Figure 1).

3. Challenges in Resin Preparation

The resins for vat photopolymerization 3D printing are mainly composed of photopolymers or monomers, photoinitiators, and diluents (reactive or nonreactive), as well as small amounts of dyes as light absorbers and radical inhibitors to prevent premature crosslinking.^[14–16] With the exception of a few reports describing degradable monomers based on small molecules with hydrolytically labile linkers,^[38,39] photoreins used for 3D printing of biodegradable implants are often prepared from synthetic photopolymers. These are in most cases based on polyesters synthesized by metal-catalyzed ring-opening polymerization (ROP), such as poly(lactide) (PLA),^[40,41] poly(ϵ -caprolactone) (PCL)^[42,43] and poly(trimethylene carbonate) (PTMC) (Scheme 1).^[44,45] The reasons are that i) ROP offers controlled synthesis of degradable polyesters with well-defined structure and tunable chain length,^[46,47] ii) the resulting polymers can be easily functionalized with photocrosslinkable groups (e.g., methacrylates), and iii) several of commonly used polyesters are already found in commercial biomedical products.^[48]

Degradable polymers obtained by polycondensation (e.g., poly(glycerol sebacate)) also show great potential in vat photopolymerization.^[49–51] However, the manipulation of their structure and molecular weight (MW) is difficult because of the nature of step-growth polymerization that requires perfect stoichiometric balance of two difunctional monomers. Photopolymers derived from natural polymers (e.g., gelatin methacryloyl) have also been investigated for 3D printing, but they provide generally weak structures, and are usually used to prepare hydrogels due to their ionic or hydrophilic characters.^[52–54]

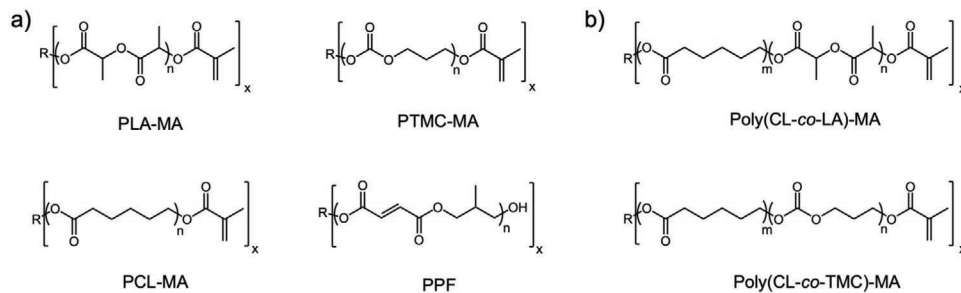
In general, a pivotal requirement for high-resolution vat photopolymerization is the low viscosity of the resins

(practically <10 Pa s)^[18,55] that enables the easy vertical detachment of the crosslinked layer from the vat film. Otherwise, the adhesive forces can cause delamination of the layers and destroy the 3D printed object. Biodegradable photopolymers often result in highly viscous resins requiring up to 50 wt% of reactive diluents (e.g., N-vinylpyrrolidone (NVP) and diethyl fumarate (DEF))^[56,57] or nonreactive solvents (e.g., propylene carbonate and ethyl lactate),^[40,58] to reduce the viscosity. In addition, the homogeneous mixing of photoinitiators (1–5 wt%) with the photopolymers also requires the assistance of organic solvents or diluents. This is because most photoinitiators used in 3D printing, in particular monoacylphosphane oxide (MAPO) and bisacylphosphane oxide (BAPO),^[59] have rigid aromatic structures and thus show limited compatibility with biodegradable photopolymers.

Although needed, solvents and reactive diluents are also introducing additional issues. Removing the volatile organic solvents (e.g., chloroform) before the printing process carries the risk of undesired premature crosslinking, while postprinting removal can cause a shrinkage of the 3D printed object.^[60] On the other hand, the addition of reactive diluents may change the structure of the crosslinked network, its crosslinking density,^[57] and increase the nondegradable part of the 3D printed devices, as these diluents are usually vinyl-based monomers. It is also commonly observed that high amounts of reactive diluents/oligomers result in brittle 3D printed products.^[61] Therefore, the preparation of biodegradable resin with low amounts or without diluents/solvents is highly desired for 3D printing but rather challenging.

4. Challenges in Printing Performance

After the optimization of the resin preparation, the printing performance of the biodegradable resins, including printability, mechanical performance, and biodegradability, need to be assessed. In 2000, Matsuda and co-workers reported the first SLA printing of biodegradable photopolymers, using a liquid copolymer synthesized from ϵ -caprolactone (CL) and trimethylene carbonate (TMC).^[25] They obtained a series of copolymers with MW ranging from 2500 to 12 000 g mol⁻¹. They did a preliminary photopatterning test with a 5100 g mol⁻¹ polymer and further 3D printed biodegradable microneedles with the polymers with MW of around 3000 g mol⁻¹, likely because polymers with higher MW were very viscous and thus difficult to print.^[62] The authors did not report the mechanical properties of the



Scheme 1. Chemical structures of representative ROP-synthesized biodegradable photopolymers based on a) homopolymers and b) copolymers. Methacrylate is the typical photocrosslinking group. m or n represents the degree of polymerization and x is the arm number of the polymers ($x = 2-4$).

3D printed products, but it is known that crosslinked networks from low MW poly(CL-co-TMC) have low mechanical strength (< 1.0 MPa).^[63] Subsequently, a number of ROP-synthesized polyester homopolymers were investigated in SLA or DLP 3D printing, including PTMC, PLA, and PCL. However, owing to the fact that the polymers with relatively higher MW are in solid state, the 3D printable resins usually consist of oligomers of less than 3000 g mol⁻¹, even when high amounts of diluents were used (up to 50 wt%).^[40–45] As a result, the 3D printed products were rather brittle with very low strain at break (typically < 50%), and thus may only be applied as tissue scaffolds that do not require high mechanical performance.

Poly(propylene fumarate) (PPF) represents another type of biodegradable photopolymer (Scheme 1).^[57,64] It bears unsaturated double bonds on the polymer backbone, alleviating the need to introduce additional crosslinking groups by postfunctionalization for 3D printing. Becker and co-workers developed a ROP method to synthesize well-defined PPF using magnesium 2,6-di-tert-butyl phenoxide as a catalyst, which produced printable photopolymers with high end-group fidelity.^[65] The DLP printed PPF scaffold was further modified with cell adhesive peptides by postprinting functionalization, to afford notable bioactivity. However, the 3D printing of PPF was still based on oligomers (MW < 3000 g mol⁻¹) and required high concentration of diluents (up to 50 wt%).^[66] Therefore, the viscosity limitation for vat photopolymerization remained the bottleneck in the optimization of the mechanical properties of the 3D printed products.

Recently, the same group designed a series of four-arm PPF polymers, with much lower viscosity compared to the linear analogs.^[67] The PPF with 200 repeating units (MW 31 000 g mol⁻¹) was successfully printed by DLP in the presence of 50 wt% DEF as a reactive diluent. Biodegradable and relatively elastic porous scaffolds with high printing quality and shape-memory behavior were obtained. The authors did not measure the tensile mechanical properties, making a comparison with other photopolymer systems difficult. Interestingly, despite the high crosslinking density caused by 50 wt% DEF, the 3D printed scaffolds exhibited significant weight loss (20–30 wt%) in 0.1 M NaOH solution after 40 days. However, the degradation behavior of the 3D printed products under physiological conditions or in vivo was not evaluated.^[67]

Although the viscosity of biodegradable photopolymers can be reduced to some extent by manipulating the polymer chain length and topology (e.g., star or branched structures), it is difficult to tackle this issue only by material design. As most of the biodegradable photopolymers are semicrystalline or amorphous, their viscosity can be substantially decreased by raising the temperature during the printing process, thereby reducing the need for high amounts of diluents.

5. Heat-Assisted Vat Photopolymerization

Recently, new opportunities have arisen with the emergence of heat-assisted vat photopolymerization (Figure 2b).^[27,68,69] Sepälä and co-workers employed heat during the SLA 3D printing of PCL tissue scaffolds in 2011.^[42] With working temperatures around 43–46 °C, they carried out the solvent-free 3D printing

of PCL methacrylate with MW of 1550 g mol⁻¹. Although the photoinitiator (Irgacure 369, 5 wt%) was dissolved in chloroform for resin preparation, no solvent nor diluent was used during the printing process as chloroform was evaporated before printing. Still, it is not possible to print photopolymers with high MW in this range of temperatures.

In 2016, Magdassi, Cohn and co-workers reported the first 3D printing of PCL methacrylate with MW of 10 000 g mol⁻¹ (melting point ≈ 50 °C) by SLA equipped with a customized heating bath.^[27] Due to the semicrystalline nature of PCL, various shape-memory complex structures, including a meshed vascular stent, could be successfully printed at 90 °C (Figure 3a). The 3D printed products exhibited much better mechanical properties in terms of elasticity and maximal strain compared to low MW PCL. The 3D printed specimens showed ultimate stress of about 1.5 MPa and strain at break of about 90%, which could be increased to more than 300% when heated to above the melting point of PCL. Using the same polymer, a personalized airway stent was fabricated from a tracheal model and its shape-memory behavior was demonstrated (Figure 3a, bottom).^[70] Most recently, they further improved the 3D printing materials by developing poly(propylene glycol)/PCL triblock photopolymers with MW ranging from 9700 to 13700 g mol⁻¹.^[71] The 3D printed tracheal stents exhibited largely increased flexibility due to the introduction of poly(propylene glycol) segments (typical MW of 8000 g mol⁻¹), while maintaining excellent shape-memory properties (Figure 3b).

Following the same principle, we have recently built a customized DLP printer with heating function.^[68] A series of biodegradable photopolymers obtained by the copolymerization of D,L-LA and CL with MW spanning from 1200 to 15 000 g mol⁻¹ were printed at 90 °C, with only 8 wt% NVP used to dissolve the BAPO photoinitiator (Irgacure 819). The strain at break of the 3D printed products could be tuned from 25% to 160% along with ultimate stress decreasing from 8.3 to 3.1 MPa. In order to further improve the mechanical properties of the materials, we introduced a dual-polymer strategy by combining four-arm long polymers (MW 15 000 g mol⁻¹) with linear oligomers (MW 600 g mol⁻¹). With a feeding ratio of 75/25 (w/w), the resin viscosity was significantly reduced compared to the single-polymer resin. The ultimate stress increased to about 13 MPa with elongation at break remaining higher than 100% (engineering stress and strain), benefiting from the enhanced crosslinking network. The mechanical performance of the 3D printed specimens was comparable to that of medical silicone materials for manufacturing airway stents. Subsequently, customized biodegradable airway stents with high elasticity and mechanical strength were fabricated, for the first time, by heat-assisted DLP. When tested in vivo, the stents showed good biocompatibility and bioresorption 8 weeks after insertion into rabbits' tracheas (Figure 3d). Therefore, the combination of new strategies in material design and emerged 3D printing techniques can potentially overcome the challenges in fabrication of personalized biodegradable medical devices with excellent mechanical performance.

Baker and co-workers employed heat-assisted DLP for the 3D printing of TMC- and CL-based copolymers.^[69] By adjusting the molar ratio of the two monomers, the ultimate stress of the

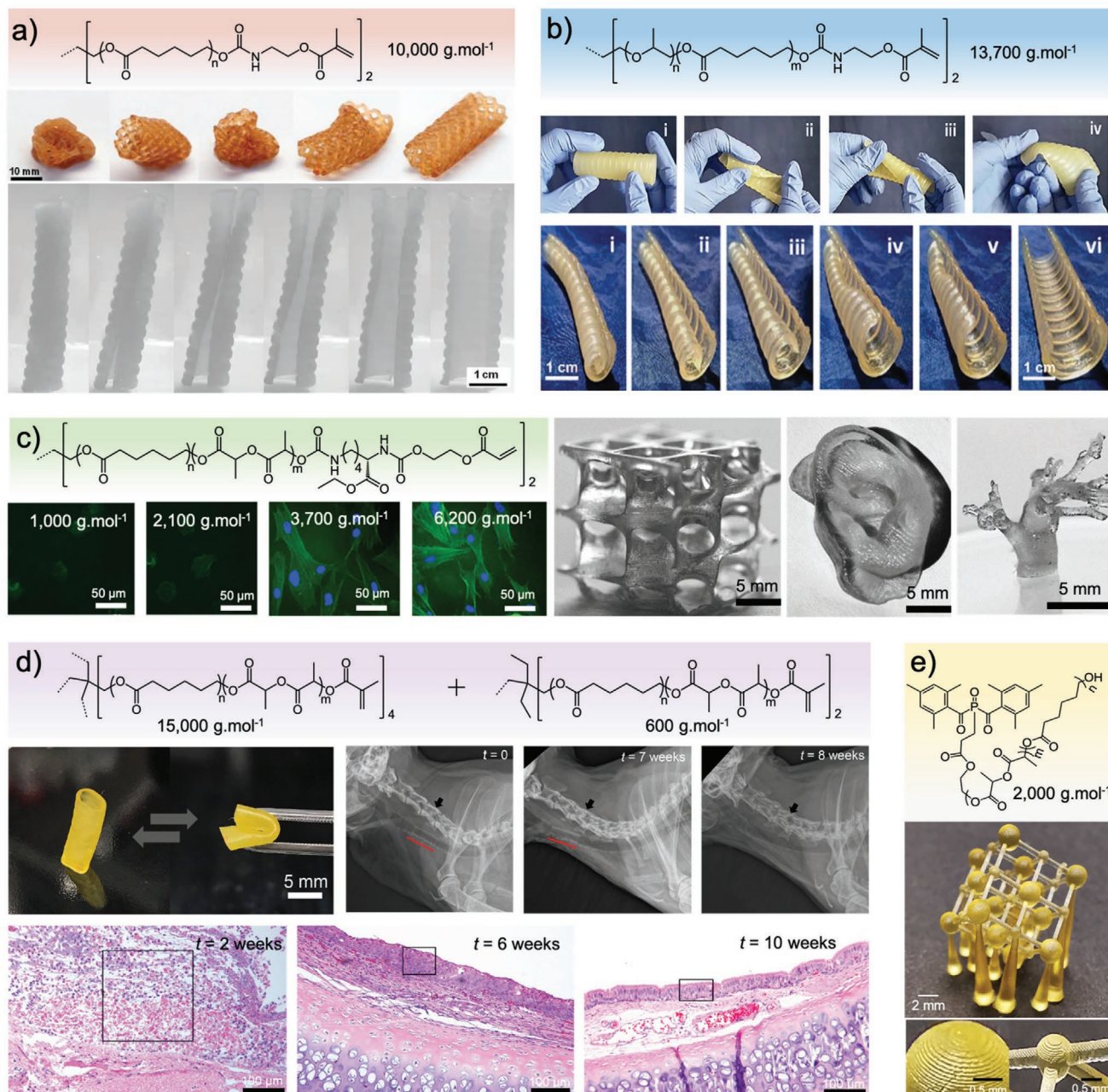


Figure 3. 3D printed biodegradable medical implants and scaffolds by heat-assisted vat photopolymerization. a) 3D printed shape-memory stent prototypes from PCL photopolymers. Reproduced with permission.^[27,70] Copyright 2016 and 2017, Wiley-VCH. b) 3D printed shape-memory tracheal stent from poly(propylene glycol)-PCL block photopolymers. Reproduced with permission.^[71] Copyright 2021, Wiley-VCH. c) 3D printed gyroid scaffolds, ear model, and vascular model from copolymers of D,L-LA and CL with varied MW, and cell staining after they were seeded on the 3D printed films at day 1. Reproduced under the terms of the CC-BY-NC-ND license.^[72] Copyright 2020, published by ChemRxiv. d) 3D printed personalized airway stents and the insertion in rabbit's trachea. The implanted stents disappeared after 8 weeks and the tracheal tissue came back to normal after 10 weeks. Reproduced under the terms of the CC-BY license.^[68] Copyright 2021, The Authors, some rights reserved; exclusive licensee American Association for the Advancement of Science. e) BAPO-based polymeric photoinitiator used to print high precision biodegradable scaffolds representing NaCl crystal lattice. Reproduced under the terms of the CC-BY-NC-ND license.^[36] Copyright 2021, The Authors, published by American Chemical Society.

photocured specimens could be tuned from 0.2 to 5.4 MPa with elongation at break of 50% to 250%. The authors claimed that the 3D printed products had slightly lower mechanical performance compared to that prepared by photocuring, albeit the experimental results were not disclosed. As the printing was

performed at only 55 °C, the MW of the polymers was limited to 3000–4000 g mol⁻¹ and 2-(2-ethoxyethoxy)ethyl acrylate was used as a reactive diluent at high concentration (30 wt%), which may explain the relatively low mechanical strength. Based on these materials, scaffolds with gyroid structure for soft tissue

regeneration were printed. Interestingly, the higher TMC fraction in the polymer network promoted a better cell adhesion. Recently, the same group developed a series of liquid photocopolymers from D,L-LA and CL with MW ranging from 1000 to 10 000 g mol⁻¹ and performed the heat-assisted DLP 3D printing at 80 °C.^[72] They reported a MW-dependent elasticity and mechanical strength of the 3D printed products. The stress at break was only in the range of 0.5–2.7 MPa, likely due to the linear polymer structure and high amount of diluent used (30 wt%). It was found that the high MW polymer-based networks (> 4000 g mol⁻¹) provide higher cell adhesion and proliferation (Figure 3c).

Clearly, heat-assisted vat photopolymerization is providing new opportunities to investigate structure–property relationships of biodegradable polymeric 3D printing materials. It permits the manufacturing of biodegradable medical devices from the highly viscous photopolymers that are not printable by conventional techniques. In fact, heat-assisted vat photopolymerization has been commercialized recently by Cubicure (cofounded by Stampfl and co-workers), and is referred to as hot lithography.^[28] This technique enables DLP 3D printing at temperatures up to 120 °C,^[73,74] allowing higher double-bond conversion and resulting in higher tensile strength and elastic modulus of 3D printed objects while maintaining high resolution. Recently, Moroni and co-workers developed a low-cost heating stage, which can be easily implemented within a commercial DLP printer.^[29]

6. Volumetric Printing

Despite its many advantages, heat-assisted vat photopolymerization has limitations when the resin viscosity exceeds the printable range even at elevated temperature. New 3D printing techniques that can overcome this important limit are highly desired. Volumetric printing based on tomographic reconstruction represents such a breakthrough in the field of vat photopolymerization.^[31–33] In 2019, Taylor and co-workers introduced a computed axial lithography technique that allowed the ultrafast fabrication of arbitrary geometries volumetrically through photopolymerization.^[31] This was achieved through concurrent printing of all points within a 3D object by illuminating a rotating volume of photosensitive material with a dynamically evolving light pattern (Figure 2c). Completely abandoning the traditional layer-by-layer stacking, volumetric 3D printing can circumvent support structures and allow printing with highly viscous fluids or even

solids, but only if they are transparent. Shortly after, Moser and co-workers improved the printing resolution to 80 μm, which is close to the values achieved with conventional SLA or DLP printers.^[32] We expect that this technique will further facilitate the development of biodegradable 3D printing materials, especially for the photopolymers with viscosity beyond the printable range of heat-assisted vat photopolymerization.

Hecht and co-workers proposed another type of volumetric printing strategy called xolography.^[34] Different from the principle of tomographic volumetric 3D printing using single light, xolography employs a dual color technique that relies on photoswitchable photoinitiators. It induces local polymerization inside a confined monomer volume upon linear excitation by intersecting light beams of different wavelengths (Figure 2d). Due to the unique two wavelength-triggered radical generation, the molecular photoswitch enables fine spatial control of the photopolymerization. Also suitable for highly viscous photopolymerization resins, this technique provides much higher resolution (≈25 μm) than tomographic volumetric printing. Importantly, the concentration of the photoswitch (0.01 wt%) is much lower than the photoinitiator concentration in conventional SLA or DLP resins (1–5 wt%). This is particularly interesting for biomedical applications of 3D printed materials as it could mitigate the potential safety concerns related to photolysis products of traditional photoinitiators. As both volumetric printing techniques require high resin viscosity to prevent sedimentation of the 3D printed solid object, long-chain biodegradable photopolymers may find their place in the rapid manufacturing of implantable devices.

A drawback of volumetric printing is that only transparent resins can be used. This is to ensure minimal diffraction and a homogenous light dose independent from penetration depth. In addition, the printable size of the object is relatively small compared to other techniques. Due to the new requirements (e.g., transparency) for the range of compatible photopolymers and the technology's novelty, volumetric printers are not yet established and thus are less accessible than conventional SLA and DLP printers. Therefore, heat-assisted vat photopolymerization will probably remain the dominant 3D printing technique in the close future, especially due to its capability to print liquid photopolymers with low transparency and semicrystalline photopolymers that are solids at room temperature (e.g., PCL-MA). For better comparison, we summarized the main features and limitations of the aforementioned 3D printing techniques as shown in **Table 1**.

Table 1. Main features and limitations of vat photopolymerization techniques for manufacturing biodegradable 3D printed medical devices.

Technique	Conventional SLA/DLP	Heat-assisted SLA/DLP	Tomographic volumetric printing	Linear volumetric printing
Resolution [μm]	30–100 ^[75]	30–100 ^{a)}	80–300 ^[32]	≈25 ^[34]
Viscosity [Pa s]	0.25–10 ^[18]	<10 at 80–100 °C ^{a)}	4–93 ^[32]	10–80 ^{b)}
Highest MW photopolymers tested	PPF (31 000 g mol ⁻¹) with 50 wt% DEF ^[67]	Poly(CL-co-DLLA)-MA (15 000 g mol ⁻¹) with 8 wt% NVP ^[68]	NA	NA
Limitations	Low viscosity Limited speed ^{c)}	Limited speed ^{c)}	High transparency Limited size ^{d)}	High transparency Limited size ^{d)}

^{a)}Estimated value in theory and from the literature (refs. [68–74]); ^{b)}Obtained from the information sheet of xolo GmbH; ^{c)}Average 20–35 mm h⁻¹ for commercial DLP printers obtained from gorillaoutput.com; ^{d)}Currently only for small objects in the centimeter range; NA: not available.

7. Polymeric Photoinitiators

As mentioned above, heat-assisted DLP and volumetric printing provide the possibility to 3D print biodegradable devices with small amounts of solvents or diluents. However, solvents or diluents are still necessary to facilitate the resin preparation and 3D printing because most photoinitiators are solids that need to be dissolved in the resin. For example, BAPO photoinitiator (Omnicure 819, previous trade name Irgacure 819) has become one of the most commonly used photoinitiators in SLA and DLP, owing to its high absorption in the visible light region^[59,76] which is particularly important for the 3D printing of biodegradable photopolymers with high chain length and hence lower crosslinking density. However, BAPO has a melting point of ≈ 130 °C, as well as limited solubility and compatibility with the resin, even when photopolymers are in a liquid state.

Grützmacher and co-workers designed a BAPO-based molecule, namely bis(mesityl)phosphane (BAP-H), which can be derivatized into various functional photoinitiator molecules.^[77] A short poly(ethylene glycol) (PEG)-conjugated photoinitiator was prepared by efficient phospho-Michael addition of BAP-H to PEG methyl ether methacrylate (MW 950 g mol⁻¹).^[78] The resulting BAPO-PEG had good water solubility and strong absorption in the visible light region, which enabled high-precision 3D printing of PEG hydrogels under blue light (460 nm) with 0.7 wt% of photoinitiator. The calculated concentration of BAPO molecule alone was lower than 0.2 wt%. Interestingly, the melting point of BAPO-PEG was only 35 °C due to the short PEG chain.^[59] This strategy is one step closer to solvent-free 3D printing resins and subsequent solvent-free biodegradable polymeric implants fabricated by heat-assisted DLP.

Inspired by this work, we synthesized biodegradable polymeric photoinitiators with MW around 2000 g mol⁻¹ using BAPO-initiated ROP of D,L-LA and CL.^[36] The initiators were liquid at room temperature and thus easily miscible with the biodegradable photopolymers based on D,L-LA and CL, allowing solvent-free manufacturing of biodegradable elastomers by heat-assisted DLP (Figure 3e). Importantly, the macrophotoinitiators enabled a systematic investigation of structure-mechanical property relationships of the photopolymers with MW in the range 1200–9100 g mol⁻¹, avoiding the interference from reactive diluents commonly used in vat photopolymerization. With only 0.5 wt% of BAPO, the 3D printed biodegradable elastomers showed good cytocompatibility and MW-dependent in vitro degradation profiles. Although the solvent-free resins for high-quality printing were limited to the photopolymers of lower viscosity with MW up to 9100 g mol⁻¹, polymers of higher MW may be potentially printable by volumetric printing as the photopolymers and macrophotoinitiators were transparent. Thanks to the advanced heat-assisted DLP, PCL-based biodegradable shape-memory scaffolds could also be printed in the presence of these liquid macrophotoinitiators.

8. Conclusions and Outlook

3D printed biodegradable medical devices have been successfully employed in medicine and have already shown their life-saving potential, exemplified by personalized PCL splints for

the treatment of severe tracheomalacia.^[79–81] Due to its superior printing quality and rapid fabrication, vat photopolymerization is expected to greatly accelerate the development of personalized implantable devices. The antagonism between the low viscosity of the resin required for high-resolution 3D printing and the high viscosity needed to confer high mechanical strength has, however, been an obstacle to the implementation of this printing method in the biomedical field. To tackle this challenge, novel strategies are required both from a material and a technological perspective:

- i) 3D printing material design: In order to obtain implants with suitable mechanical properties and degradation profiles, it is essential to focus on the design of photopolymers with high MW. While long degradable chains bring elasticity and degradability to the system, relatively high crosslinking density is needed for sufficient mechanical strength. Dual-polymer resins combining long and short photopolymers could be a convenient solution to achieve a balance among different key properties (e.g., elasticity and strength) and simultaneously reduce the viscosity. In addition, more synthetic routes for biodegradable photopolymers should be explored. For example, the photopolymerizable groups can be introduced by the side-group functionalization of ROP monomers, allowing the control of the photocrosslinkable sites in the resulting polymers.^[82,83] More polymeric topologies (i.e., bottlebrush and hyperbranched polymers) that are rarely reported for photopolymerization 3D printing but exhibit potentially low intrinsic viscosity could also be investigated.^[84,85] Random and block copolymerizations can provide various opportunities for further tuning the mechanical properties of the crosslinked networks. In addition to rational chemical design, machine learning and data mining^[86,87] are useful tools. By integrating the viscosities, mechanical properties, and degradation behaviors of the reported photopolymers developed either for conventional photopolymerization or for 3D printing, these tools could generate a material database and help predicting 3D-printable biodegradable structures with the most promising properties in specific applications. This might reduce the workload for the development of new 3D printing materials, especially when considering photopolymerization, 3D printing tests can consume a relatively large amount of synthetic materials. Furthermore, various biodegradable polymeric photoinitiators could be designed through photoinitiator-initiated ROP or postconjugation to improve compatibility with the photopolymers. Numerous polymeric photoinitiators that have been reported in literature but have not yet been applied to vat photopolymerization^[88,89] may be worth revisiting to evaluate their potential in 3D printing.
- ii) 3D printing technique selection: In general, heat-assisted vat photopolymerization is highly efficient to print amorphous liquid photopolymers or semicrystalline photopolymers with a low melting point. So far, heat-assisted vat photopolymerization has allowed the high precision manufacturing of implantable devices or scaffolds with tunable mechanical performance and degradability, while the fabrication of biodegradable materials by volumetric printing has not yet been reported. When the resin viscosity exceeds the workable limit for heat-assisted SLA or DLP, volumetric printing would

show its superiority, but the high-transparency requirement for 3D printing resins and the limitation in printable size are challenges to be considered. New printing techniques that can combine the merits of both methods would be highly desired. CLIP at elevated temperature has not yet been reported, likely due to its lower accessibility compared to SLA or DLP. In addition, the oxygen permeability–heat relationship will have to be investigated for the optimization of the 3D printing performance. If a CLIP printer can be equipped with a heating function, the fabrication of biodegradable medical devices could be much faster and more efficient.

Overall, significant progress in the development of biodegradable medical devices or implants by vat photopolymerization has been achieved. With increasing complexity, the translation of these devices/implants toward clinical applications will be a challenge, but also a driving force for multidisciplinary research involving chemistry, material science, mechanical engineering, pharmaceutical science, veterinary and human medicine. On the basis of ongoing advancements in both novel materials and high precision 3D printing techniques, photopolymerization 3D printing may eventually revolutionize the manufacturing of biodegradable medical implants or devices and become an irreplaceable tool in personalized medicine.

Acknowledgements

The Swiss National Science Foundation is acknowledged for financial support (Sinergia No. 177178). Dr. Valeria Mantella, Dr. Angela Steinauer, and Dr. Adva Krivitsky (ETH Zurich) are acknowledged for the critical reading of the manuscript. Dr. Niklas Felix König (xolo GmbH) is acknowledged for providing the information sheet and suggestions on the paragraphs about volumetric printing.

Open access funding provided by Eidgenössische Technische Hochschule Zurich.

Conflict of Interest

The authors declare no conflict of interest.

Keywords

3D printing, biodegradable, digital light processing, medical devices, photopolymerization, volumetric printing

Received: September 29, 2021

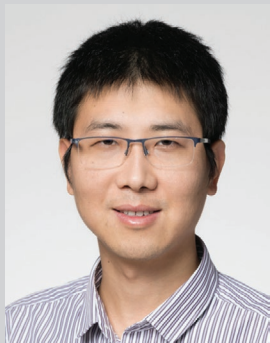
Revised: December 21, 2021

Published online: January 19, 2022

- [1] C. Li, C. Guo, V. Fitzpatrick, A. Ibrahim, M. J. Zwierstra, P. Hanna, A. Lechtig, A. Nazarian, S. J. Lin, D. L. Kaplan, *Nat. Rev. Mater.* **2020**, *5*, 61.
- [2] Y. Khan, A. E. Ostfeld, C. M. Lochner, A. Pierre, A. C. Arias, *Adv. Mater.* **2016**, *28*, 4373.
- [3] J. J. Wykrzykowska, R. P. Kraak, S. H. Hofma, R. J. Van Der Schaaf, E. K. Arkenbout, A. J. IJsselmuiden, J. Elias, I. M. Van Dongen, R. Y. G. Tijssen, K. T. Koch, J. Baan, M. M. Vis, R. J. De Winter,

- J. J. Piek, J. G. P. Tijssen, J. P. S. Henriques, *N. Engl. J. Med.* **2017**, *376*, 2319.
- [4] H. Dutau, A. I. Musani, S. Laroumagne, K. Darwiche, L. Freitag, P. Astoul, *Respiration* **2015**, *90*, 512.
- [5] R. Farra, N. F. Sheppard, L. McCabe, R. M. Neer, J. M. Anderson, J. T. Santini, M. J. Cima, R. Langer, *Sci. Transl. Med.* **2012**, *4*, 122ra21.
- [6] R. Agarwal, A. J. García, *Adv. Drug Delivery Rev.* **2015**, *94*, 53.
- [7] A. S. Mao, D. J. Mooney, *Proc. Natl. Acad. Sci. USA* **2015**, *112*, 14452.
- [8] R. Singh, M. J. Bathaei, E. Istif, L. Beker, *Adv. Healthcare Mater.* **2020**, *9*, 2000790.
- [9] U. Sharma, D. Concagh, L. Core, Y. Kuang, C. You, Q. Pham, G. Zugates, R. Busold, S. Webber, J. Merlo, R. Langer, G. M. Whitesides, M. Palasis, *Nat. Mater.* **2018**, *17*, 96.
- [10] G. Haghiashtiani, K. Qiu, J. D. Z. Sanchez, Z. J. Fuenning, P. Nair, S. E. Ahlberg, P. A. Iazzo, M. C. McAlpine, *Sci. Adv.* **2020**, *6*, eabb4641.
- [11] M. Schaffner, P. A. Rühls, F. Coulter, S. Kilcher, A. R. Studart, *Sci. Adv.* **2017**, *3*, eaao6804.
- [12] J. Koffler, W. Zhu, X. Qu, O. Platoshyn, J. N. Dulin, J. Brock, L. Graham, P. Lu, J. Sakamoto, M. Marsala, S. Chen, M. H. Tuszynski, *Nat. Med.* **2019**, *25*, 263.
- [13] J. U. Lind, T. A. Busbee, A. D. Valentine, F. S. Pasqualini, H. Yuan, M. Yadid, S. Park, A. Kotikian, A. P. Nesmith, P. H. Campbell, J. J. Vlassak, J. A. Lewis, K. K. Parker, *Nat. Mater.* **2017**, *16*, 303.
- [14] C. Yu, J. Schimelman, P. Wang, K. L. Miller, X. Ma, S. You, J. Guan, B. Sun, W. Zhu, S. Chen, *Chem. Rev.* **2020**, *120*, 10695.
- [15] A. Bagheri, J. Jin, *ACS Appl. Polym. Mater.* **2019**, *1*, 593.
- [16] X. Xu, A. Awad, P. Robles-Martinez, S. Gaisford, A. Goyanes, A. W. Basit, *J. Controlled Release* **2021**, *329*, 743.
- [17] F. P. W. Melchels, J. Feijen, D. W. Grijpma, *Biomaterials* **2010**, *31*, 6121.
- [18] R. J. Mondschein, A. Kanitkar, C. B. Williams, S. S. Verbridge, T. E. Long, *Biomaterials* **2017**, *140*, 170.
- [19] S. H. Kim, Y. K. Yeon, J. M. Lee, J. R. Chao, Y. J. Lee, Y. B. Seo, M. T. Sultan, O. J. Lee, J. S. Lee, S.-I. Yoon, I.-S. Hong, G. Khang, S. J. Lee, J. J. Yoo, C. H. Park, *Nat. Commun.* **2018**, *9*, 1620.
- [20] X. Kuang, J. Wu, K. Chen, Z. Zhao, Z. Ding, F. Hu, D. Fang, H. J. Qi, *Sci. Adv.* **2019**, *5*, eaav5790.
- [21] J. R. Tumbleston, D. Shirvanyants, N. Ermoshkin, R. Januszewicz, A. R. Johnson, D. Kelly, K. Chen, R. Pinschmidt, J. P. Rolland, A. Ermoshkin, E. T. Samulski, J. M. DeSimone, *Science* **2015**, *347*, 1349.
- [22] H. J. Oh, M. S. Aboian, M. Y. J. Yi, J. A. Maslyn, W. S. Loo, X. Jiang, D. Y. Parkinson, M. W. Wilson, T. Moore, C. R. Yee, G. R. Robbins, F. M. Barth, J. M. Desimone, S. W. Hetts, N. P. Balsara, *ACS Cent. Sci.* **2019**, *5*, 419.
- [23] B. Grigoryan, S. J. Paulsen, D. C. Corbett, D. W. Sazer, C. L. Fortin, A. J. Zaita, P. T. Greenfield, N. J. Calafat, J. P. Gounley, A. H. Ta, F. Johansson, A. Randles, J. E. Rosenkrantz, J. D. Louis-Rosenberg, P. A. Galie, K. R. Stevens, J. S. Miller, *Science* **2019**, *364*, 458.
- [24] R. Gauvin, Y.-C. Chen, J. W. Lee, P. Soman, P. Zorlutuna, J. W. Nichol, H. Bae, S. Chen, A. Khademhosseini, *Biomaterials* **2012**, *33*, 3824.
- [25] T. Matsuda, M. Mizutani, S. C. Arnold, *Macromolecules* **2000**, *33*, 795.
- [26] K. Liang, S. Carmone, D. Brambilla, J. C. Leroux, *Sci. Adv.* **2018**, *4*, eaat2544.
- [27] M. Zarek, M. Layani, I. Cooperstein, E. Sachyani, D. Cohn, S. Magdassi, *Adv. Mater.* **2016**, *28*, 4449.
- [28] B. Steyrer, B. Buseti, G. Harakály, R. Liska, J. Stampfl, *Addit. Manuf.* **2018**, *21*, 209.
- [29] T. Kuhnt, F. L. C. Morgan, M. B. Baker, L. Moroni, *Addit. Manuf.* **2021**, *46*, 102102.
- [30] M. Shusteff, A. E. M. Browar, B. E. Kelly, J. Henriksson, T. H. Weisgraber, R. M. Panas, N. X. Fang, C. M. Spadaccini, *Sci. Adv.* **2017**, *3*, eaao5496.

- [31] B. E. Kelly, I. Bhattacharya, H. Heidari, M. Shusteff, C. M. Spadaccini, H. K. Taylor, *Science* **2019**, *363*, 1075.
- [32] D. Loterie, P. Delrot, C. Moser, *Nat. Commun.* **2020**, *11*, 852.
- [33] P. N. Bernal, P. Delrot, D. Loterie, Y. Li, J. Malda, C. Moser, R. Levato, *Adv. Mater.* **2019**, *31*, 1904209.
- [34] M. Regehly, Y. Garmshausen, M. Reuter, N. F. König, E. Israel, D. P. Kelly, C. Y. Chou, K. Koch, B. Asfari, S. Hecht, *Nature* **2020**, *588*, 620.
- [35] M. Brooks, *New Sci.* **2016**, *232*, 40.
- [36] M. Sandmeier, N. Paunović, R. Conti, L. Hofmann, J. Wang, Z. Luo, K. Masania, N. Wu, N. Kleger, F. B. Coulter, A. R. Studart, H. Grützmacher, J.-C. Leroux, Y. Bao, *Macromolecules* **2021**, *54*, 7830.
- [37] D. A. Walker, J. L. Hedrick, C. A. Mirkin, *Science* **2019**, *366*, 360.
- [38] C. Heller, M. Schwentenwein, G. Russmüller, T. Koch, D. Moser, C. Schopper, F. Varga, J. Stampfl, R. Liska, *J. Polym. Sci., Part A: Polym. Chem.* **2011**, *49*, 650.
- [39] A. Oesterreicher, J. Wiener, M. Roth, A. Moser, R. Gmeiner, M. Edler, G. Pinter, T. Griesser, *Polym. Chem.* **2016**, *7*, 5169.
- [40] F. P. W. Melchels, J. Feijen, D. W. Grijpma, *Biomaterials* **2009**, *30*, 3801.
- [41] J. Jansen, F. P. W. Melchels, D. W. Grijpma, J. Feijen, *Biomacromolecules* **2009**, *10*, 214.
- [42] L. Elomaa, S. Teixeira, R. Hakala, H. Korhonen, D. W. Grijpma, J. V. Seppälä, *Acta Biomater.* **2011**, *7*, 3850.
- [43] B. J. Green, K. S. Worthington, J. R. Thompson, S. J. Bunn, M. Rethwisch, E. E. Kaalberg, C. Jiao, L. A. Wiley, R. F. Mullins, E. M. Stone, E. H. Sohn, B. A. Tucker, C. A. Guymon, *Biomacromolecules* **2018**, *19*, 3682.
- [44] I. K. Kwon, T. Matsuda, *Biomaterials* **2005**, *26*, 1675.
- [45] S. Schüller-Ravoo, E. Zant, J. Feijen, D. W. Grijpma, *Adv. Healthcare Mater.* **2014**, *3*, 2004.
- [46] G. Becker, F. R. Wurm, *Chem. Soc. Rev.* **2018**, *47*, 7739.
- [47] N. E. Kamber, W. Jeong, R. M. Waymouth, R. C. Pratt, B. G. G. Lohmeijer, J. L. Hedrick, *Chem. Rev.* **2007**, *107*, 5813.
- [48] C. Jérôme, P. Lecomte, *Adv. Drug Delivery Rev.* **2008**, *60*, 1056.
- [49] R. van Lith, E. Baker, H. Ware, J. Yang, A. C. Farsheed, C. Sun, G. Ameer, *Adv. Mater. Technol.* **2016**, *1*, 1600138.
- [50] P. Wang, D. B. Berry, Z. Song, W. Kiratitanaporn, J. Schimelman, A. Moran, F. He, B. Xi, S. Cai, S. Chen, *Adv. Funct. Mater.* **2020**, *30*, 1910391.
- [51] I. Louzao, B. Koch, V. Taresco, L. Ruiz-Cantu, D. J. Irvine, C. J. Roberts, C. Tuck, C. Alexander, R. Hague, R. Wildman, M. R. Alexander, *ACS Appl. Mater. Interfaces* **2018**, *10*, 6841.
- [52] W. Zhu, K. R. Tringale, S. A. Woller, S. You, S. Johnson, H. Shen, J. Schimelman, M. Whitney, J. Steinauer, W. Xu, T. L. Yaksh, Q. T. Nguyen, S. Chen, *Mater. Today* **2018**, *21*, 951.
- [53] W. Li, L. S. Mille, J. A. Robledo, T. Uribe, V. Huerta, Y. S. Zhang, *Adv. Healthcare Mater.* **2020**, *9*, 2000156.
- [54] S. Bose, C. Koski, A. A. Vu, *Mater. Horiz.* **2020**, *7*, 2011.
- [55] S. Schüller-Ravoo, S. M. Teixeira, J. Feijen, D. W. Grijpma, A. A. Poot, *Macromol. Biosci.* **2013**, *13*, 1711.
- [56] S. C. Ligon, R. Liska, J. Stampfl, M. Gurr, R. Mülhaupt, *Chem. Rev.* **2017**, *117*, 10212.
- [57] M. N. Cooke, J. P. Fisher, D. Dean, C. Rimnac, A. G. Mikos, *J. Biomed. Mater. Res., Part B* **2003**, *64*, 65.
- [58] B. van Bochove, G. Hannink, P. Buma, D. W. Grijpma, *Macromol. Biosci.* **2016**, *16*, 1853.
- [59] J. Wang, *Doctoral Thesis*, Synthesis and Application of Bis(acyl) phosphane Oxide Photoinitiators, ETH Zurich, **2017**.
- [60] H. Quan, T. Zhang, H. Xu, S. Luo, J. Nie, X. Zhu, *Bioact. Mater.* **2020**, *5*, 110.
- [61] J. Zhang, P. Xiao, *Polym. Chem.* **2018**, *9*, 1530.
- [62] T. Matsuda, M. Mizutani, *J. Biomed. Mater. Res.* **2002**, *62*, 395.
- [63] L.-Q. Yang, B. He, S. Meng, J.-Z. Zhang, M. Li, J. Guo, Y.-M. Guan, J.-X. Li, Z.-W. Gu, *Polymer* **2013**, *54*, 2668.
- [64] Y. Luo, C. K. Dolder, J. M. Walker, R. Mishra, D. Dean, M. L. Becker, *Biomacromolecules* **2016**, *17*, 690.
- [65] J. A. Wilson, D. Luong, A. P. Kleinfehn, S. Sallam, C. Wesdemiotis, M. L. Becker, *J. Am. Chem. Soc.* **2018**, *140*, 277.
- [66] Y. Luo, G. L. Fer, D. Dean, M. L. Becker, *Biomacromolecules* **2019**, *20*, 1699.
- [67] G. L. Fer, M. L. Becker, *ACS Appl. Mater. Interfaces* **2020**, *12*, 22444.
- [68] N. Paunović, Y. Bao, F. B. Coulter, K. Masania, A. Karoline, K. Klein, A. Rafsanjani, J. Cadalbert, P. W. Kronen, A. Karol, Z. Luo, F. Rüber, D. Brambilla, B. Von, D. Franzen, A. R. Studart, J.-C. Leroux, *Sci. Adv.* **2021**, *7*, abe9499.
- [69] T. Kuhnt, R. Marroquín García, S. Camarero-Espinosa, A. Dias, A. T. Ten Cate, C. A. Van Blitterswijk, L. Moroni, M. B. Baker, *Biomater. Sci.* **2019**, *7*, 4984.
- [70] M. Zarek, N. Mansour, S. Shapira, D. Cohn, *Macromol. Rapid Commun.* **2017**, *38*, 1600628.
- [71] N. Maity, N. Mansour, P. Chakraborty, D. Bychenko, E. Gazit, D. Cohn, *Adv. Funct. Mater.* **2021**, *31*, 2108436.
- [72] M. Baker, R. Wang, F. Damanik, T. Kuhnt, H. Ippel, P. Dijkstra, T. ten Cate, A. Dias, L. Moroni, **2020**, <https://doi.org/10.26434/chemrxiv.12053037.v1>.
- [73] M. Pfaffinger, *Laser Tech. J.* **2018**, *15*, 45.
- [74] N. Kikivits, L. Sinawehl, P. Knaack, T. Koch, J. Stampfl, C. Gorsche, R. Liska, *ACS Macro Lett.* **2020**, *9*, 546.
- [75] L. Moroni, T. Boland, J. A. Burdick, C. De Maria, B. Derby, G. Forgacs, J. Groll, Q. Li, J. Malda, V. A. Mironov, C. Mota, M. Nakamura, W. Shu, S. Takeuchi, T. B. F. Woodfield, T. Xu, J. J. Yoo, G. Vozzi, *Trends Biotechnol.* **2018**, *36*, 384.
- [76] K. Sun, Y. Xu, F. Dumur, F. Morlet-Savary, H. Chen, C. Dietlin, B. Graff, J. Lalevé, P. Xiao, *Polym. Chem.* **2020**, *11*, 2230.
- [77] J. Wang, A. Chiappone, I. Roppolo, F. Shao, E. Fantino, M. Lorusso, D. Rentsch, K. Dietliker, C. F. Pirri, H. Grützmacher, *Angew. Chem., Int. Ed.* **2018**, *57*, 2353.
- [78] J. Wang, S. Stanic, A. A. Altun, M. Schwentenwein, K. Dietliker, L. Jin, J. Stampfl, S. Baudis, R. Liska, H. Grützmacher, *Chem. Commun.* **2018**, *54*, 920.
- [79] D. A. Zopf, S. J. Hollister, M. E. Nelson, R. G. Ohye, G. E. Green, *N. Engl. J. Med.* **2013**, *368*, 2043.
- [80] R. J. Morrison, S. J. Hollister, M. F. Niedner, M. G. Mahani, A. H. Park, D. K. Mehta, R. G. Ohye, G. E. Green, *Sci. Transl. Med.* **2015**, *7*, 285ra64.
- [81] U. Ghosh, S. Ning, Y. Wang, Y. L. Kong, *Adv. Healthcare Mater.* **2018**, *7*, 1800417.
- [82] A. C. Weems, M. C. Arno, W. Yu, R. T. R. Huckstepp, A. P. Dove, *Nat. Commun.* **2021**, *12*, 3771.
- [83] W. Zhu, S.-H. Pyo, P. Wang, S. You, C. Yu, J. Alido, J. Liu, Y. Leong, S. Chen, *ACS Appl. Mater. Interfaces* **2018**, *10*, 5331.
- [84] R. Xie, S. Mukherjee, A. E. Levi, V. G. Reynolds, H. Wang, M. L. Chabinyc, C. M. Bates, *Sci. Adv.* **2020**, *6*, eabc6900.
- [85] Z. Wang, J. Zhang, J. Liu, S. Hao, H. Song, J. Zhang, *ACS Appl. Mater. Interfaces* **2021**, *13*, 5614.
- [86] G. D. Goh, S. L. Sing, W. Y. Yeong, *Artif. Intell. Rev.* **2021**, *54*, 63.
- [87] M. Elbadawi, L. E. McCoubrey, F. K. H. Gavins, J. J. Ong, A. Goyanes, S. Gaisford, A. W. Basit, *Trends Pharmacol. Sci.* **2021**, *42*, 745.
- [88] J. Zhou, X. Allonas, A. Ibrahim, X. Liu, *Prog. Polym. Sci.* **2019**, *99*, 101165.
- [89] T. Corrales, F. Catalina, C. Peinado, N. S. Allen, *J. Photochem. Photobiol., A* **2003**, *159*, 103.



Yinyin Bao is a group leader in the Institute of Pharmaceutical Sciences at ETH Zürich. Dr. Bao graduated from Hefei University of Technology in 2007 and received his Ph.D. degree in Polymer Chemistry from University of Science and Technology of China in 2012. Then he completed a postdoctoral research at KU Leuven, and in 2014 became a Marie Curie IntraEuropean Fellow of CNRS at the University of Paris Sud. From 2016 he joined the group of Prof. Jean-Christophe Leroux, and he was promoted to a senior scientist position late 2018. His research interests remain light-emitting materials, drug delivery, and 3D printing.



Nevena Paunović is a Ph.D. student in the Drug Formulation and Delivery group at ETH Zurich working on a project related to biodegradable materials for 3D printing of medical devices. She is a licensed pharmacist who holds a Master in Pharmaceutical Sciences (2015) from the University of Belgrade and a Master in Drug Sciences with specialization in toxicology (2018) from the University of Basel.



Jean-Christophe Leroux is a full professor of Drug Formulation and Delivery at the Institute of Pharmaceutical Sciences at ETH Zurich, Switzerland. He has made important fundamental and applied contributions to the fields of biomaterials and drug delivery, and has been involved in the development of innovative bio-detoxification systems for the treatment of intoxications. He is a fellow of the AAPS and the CRS, and the co-founder of the start-up pharmaceutical companies Versantis AG and Inositec AG.